An Indicator Based Multi-Objective Evolutionary Algorithm with Reference Point Adaptation for Better Versatility

Ye Tian, Ran Cheng, Xingyi Zhang, Fan Cheng, and Yaochu Jin, *Fellow, IEEE*

***Abstract*—During the past two decades, a variety of multi-objective evolutionary algorithms (MOEAs) have been proposed in the literature. As pointed out in some recent studies, however, the performance of an MOEA can strongly depend on the Pareto front shape of the problem to be solved, whereas most existing MOEAs show poor versatility on problems with different shapes of Pareto fronts. To address this issue, we propose an MOEA based on an enhanced inverted generational distance indicator, in which an adaptation method is suggested to adjust a set of reference points based on the indicator contributions of candidate solutions in an external archive. Our experimental results demonstrate that the proposed algorithm is versatile for solving problems with various types of Pareto fronts, outperforming several state-of-the-art evolutionary algorithms for multi-objective and many-objective optimization.**

***Index Terms*—Evolutionary multi-objective optimization, many-objective optimization, indicator based selection, adaptive reference point**

I. Introduction

MULTI-objective optimization problems (MOPs), which involve two or more conflicting objectives to be optimized, can be formulated as follows:

$$\begin{aligned} \min_{x} \quad & F(x) = (f_1(x), ..., f_M(x)) \\ \text{s.t.} \quad & x \in X, \end{aligned} \tag{1}$$

where $X \subseteq \mathbb{R}^D$ is the decision space, $F : X \to Y \subseteq \mathbb{R}^M$ consists of M objectives and Y is the objective space. Specially, if an MOP has more than three objectives (i.e. $M > 3$), it is often known as a many-objective optimization problem (MaOP) nowadays. Due to the conflicting nature between the multiple objectives, there does not exist single optimal solution that is able to optimize all the objectives; instead, a number of solutions can be obtained as trade-offs between different objectives, known as the Pareto optimal set. To approximate the Pareto optimal set, a number of multi-objective evolutionary algorithms (MOEAs) have been developed during the past two decades, which can be roughly classified into three categories [1], [2].

The first category is the Pareto dominance based MOEAs, where Pareto dominance based mechanisms are adopted to distinguish and select candidate solutions. The NSGA-II [3], SPEA2 [4] and PESA-II [5] are three representative MOEAs of this type, where all non-dominated solutions are first identified and then a secondary strategy is used to make selections among the non-dominated solutions to preserve the population diversity. Although Pareto dominance based MOEAs have shown promising performance on MOPs with two or three objectives, their performance deteriorates rapidly as the number of objectives increases on MaOPs, mainly due to the phenomenon known as the dominance resistance [6]. To address this issue, some specially tailored Pareto dominance based MOEAs have been recently proposed for tackling MaOPs, such as the grid dominance based evolutionary algorithm (GrEA) [7] and knee point driven evolutionary algorithm (KnEA) [8], among many others [2].

The second category is the decomposition based MOEAs, where an original MOP is decomposed into a number of single-objective optimization problems (SOPs) or simpler MOPs to be solved collaboratively. On one hand, some decomposition based MOEAs such as MOGLS [9], C-MOGA [10], MSOPS-II [11], MOEA/D [12] and RVEA [13] decompose an MOP into a number of SOPs via objective function aggregations, such that the candidate solutions are able to efficiently converge to the optimum of each SOP without considering the conflicts between different objectives. On the other hand, some other decomposition based MOEAs such as MOEA/D-M2M [14], IM-MOEA [15], NSGA-III [16] and SPEA/R [17], decompose an MOP into

Manuscript received –. This work was supported in part by the National Natural Science Foundation of China under Grant 61272152, Grant 61502004, Grant 61502001 and Grant 61672033. The work of Y. Jin was supported in part by the Joint Research Fund for Overseas Chinese, Hong Kong and Macao Scholars of the National Natural Science Foundation of China under Grant 61428302, and in part by the U.K. EPSRC Under Grant EP/M017869/1. *(Corresponding author: Xingyi Zhang)*

Y. Tian, X. Zhang and F. Cheng are with the Institute of Bio-inspired Intelligence and Mining Knowledge, School of Computer Science and Technology, Anhui University, Hefei 230039, China (email: field910921@gmail.com; xyzhanghust@gmail.com; chengfan@mail.ustc.edu.cn). This work was performed when Y. Tian was visiting the Department of Computer Science, University of Surrey.

R. Cheng is with the School of Computer Science, University of Birmingham, Birmingham, B15 2TT, U.K. (email: ranchengcn@gmail.com)

Y. Jin is with the Department of Computer Science, University of Surrey, Guildford, Surrey, GU2 7XH, U.K. (email: yaochu.jin@surrey.ac.uk).

several simpler MOPs by partitioning the objective space into a number of subspaces.

The third category is the indicator based MOEAs, where performance indicators of solution quality measurement are adopted as selection criteria in the environmental selection. Representatives of this type include IBEA [18], SMS-EMOA [19], GDE-MOEA [20] and MOMBI-II [21], where the environmental selection strategies are designed based on a predefined binary indicator, the hypervolume (HV) indicator, the generational distance and the R2 indicator, respectively. The HypE proposed in [22] is also a hypervolume indicator based MOEA, where the Monter Carlo simulation is adopted to estimate the hypervolume contributions of the candidate solutions for addressing the high complexity of exact hypervolume calculation in solving MaOPs. It is worth noting that the recently proposed weakly Pareto compliant Sharpe-Ratio indicator also provides an alternative way to generalize hypervolume to many-objective optimization [23], [24].

Although most MOEAs in the literature have been verified on different types of benchmark MOPs and MaOPs, it has been pointed out in some recent studies that the performance of an MOEA can strongly depend on Pareto front shape of the problem to be solved [25], [26]. In other words, some MOEAs are more capable of dealing with regular Pareto fronts[1], while others are specially tailored for problems with irregular Pareto fronts [2]. However, the performance of most MOEAs is sensitive to Pareto front shapes. To take the decomposition based MOEAs as an example, as recently reported by Ishibuchi *et al.* in [26], good results can be obtained by these algorithms only if the distribution of weight vectors is consistent with the Pareto front shape of the problem to be solved. To address such an issue, we propose a novel indicator based MOEA, termed AR-MOEA. The main new contributions of this work are summarized as follows.

1) The enhanced inverted generational distance (IGD-NS) indicator [27] is adopted as the selection criterion in the proposed AR-MOEA. Compared to IGD, the IGD-NS indicator is capable of distinguishing solutions that have no contribution to the indicator, thus being able to accelerate the evolution of a population towards the Pareto front when it is adopted as a selection criterion in MOEAs.
2) In calculating IGD-NS, a set of reference points are adaptively maintained and updated. Considering that different types of Pareto fronts may have different shapes, the proposed reference point adaptation method not only takes advantage of points uniformly sampled from a unit hyperplane, but also adaptively adjusts the distribution of the reference points according to the contribution of candidate solutions in an external archive in terms of IGD-NS. Compared to existing reference point adaptation methods, the proposed method has better robustness in capturing different shapes of Pareto fronts. In addition, the proposed reference point adaptation method is parameterless, and can be easily deployed in other existing decomposition based MOEAs.
3) To verify the versatility of the proposed AR-MOEA, a variety of 22 test problems having various Pareto fronts are used as the testbed in the empirical studies, where the number of objectives is scaled from three to ten. In comparison with eight state-of-the-art MOEAs, experimental results demonstrate that AR-MOEA has promising versatility on MOPs and MaOPs with different types of Pareto fronts, some of which are smooth and continuous, and the others are degenerate, disconnected, inverted or with sharp tails.

The rest of this paper is organized as follows. In Section II, existing indicator based MOEAs as well as reference point adaptation strategies are briefly reviewed. The motivation of this paper is also elaborated in Section II. In Section III, the details of the proposed algorithm AR-MOEA are described and empirical results of AR-MOEA compared with existing MOEAs are presented in Section IV. Finally, conclusion and future work are given in Section V.

II. Related Work

A. Indicator Based MOEAs

In the past few years, a large number of performance indicators have been proposed in the literature, e.g., generational distance (GD) [28], inverted generational distance (IGD) [29], hypervolume (HV) [30], R2 [31], Δ_p [32], pure diversity (PD) [33] and IGD-NS [27]. Most of these indicators are not only widely used to assess the quality of solutions sets, but also applied as selection criteria in MOEAs. In the following, we briefly recall some representative indicator based MOEAs.

The first well known indicator based evolutionary algorithm is the IBEA suggested by Zitzler and Künzli in 2004 [18], where the environmental selection is designed based on a predefined binary indicator. Empirical results indicated that IBEA was superior over two popular MOEAs, NSGA-II and SPEA2, on several bi-/three-objective benchmark MOPs [18]. The main contribution of IBEA is that it provides a general framework for indicator based MOEAs, which had triggered future studies along this direction.

Another early representative work is the SMS-EMOA proposed by Beume *et al.* [19], where the HV indicator was used as the selection criterion. In spite of the competitive performance of SMS-EMOA on bi-objective MOPs in terms of HV, it is difficult to be used for solving MaOPs due to the exponentially increased computational cost of HV calculation. To address this issue,

[1]In this paper, regular Pareto fronts refer to those that are smooth, continuous and well spread.

[2]In this paper, irregular Pareto fronts refer to those that are degenerate, disconnected, inverted or with sharp tails.

Bader and Zitzler [22] suggested a fast HV based evolutionary algorithm, named HypE, for many-objective optimization. In HypE, a Monte Carlo simulation based HV estimation method is used instead of the accurate HV calculation, such that the computational efficiency of HV calculation can be substantially improved when the number of objective is large.

The POSEA is also an interesting indicator based MOEA developed by Yevseyeva *et al.* in [23], where the Sharpe-Ratio indicator was proposed based on a formulation of fitness assignment as a portfolio selection problem. In POSEA, the Sharpe-Ratio indicator is combined with the hypervolume indicator, which could provide an alternative way to generalize hypervolume to many-objective optimization. In [24], a detailed discussion on the properties of Sharpe-Ratio indicator was presented in terms of monotonicity, sensitivity to scaling and parameter independence.

There are also some MOEAs based on other performance indicators. For example, Trautmann *et al.* developed an R2 indicator in [34] for solving MOPs, and Gómez and Coello Coello proposed two extensions of R2 based MOEAs for solving MaOPs, termed MOMBI [35] and MOMBI-II [21], respectively; Menchaca-Mendez and Coello Coello proposed a GD indicator based MOEA, termed GD-MOEA [36], and an improved version GDE-MOEA [20] by incorporating the ϵ-dominance into the GD-MOEA algorithm; Rudolph *et al.* [37] developed an MOEA based on the Δ_p indictor, termed AS-MOEA, where Δ_p is a modified composition of GD and IGD [38]–[40].

Recently, an enhanced IGD indicator, called IGD with noncontributing solution detection (IGD-NS), has been proposed by us in [27]. By distinguishing the noncontributing solutions which do not have any contribution to the indicator, the IGD-NS is able to provide a more comprehensive measurement of a non-dominated solution set. Based on the IGD-NS, an algorithm named MOEA/IGD-NS has also been suggested, where the non-dominated solutions stored in an external archive are used as the reference points for the calculation of IGD-NS. Empirical results demonstrated that although MOEA/IGD-NS outperformed several existing MOEAs on some MOPs with two or three objectives, the algorithm has poor versatility on problems with different types of Pareto fronts, and it also has difficulty in tackling problems with more than three objectives, namely, MaOPs. To address this issue, we propose a novel IGD-NS based MOEA with better versatility in this paper, termed AR-MOEA, where a reference point adaptation method is developed to adjust the reference points for the calculation of IGD-NS at each generation.

B. Reference Point Adaptation Methods

For the calculation of many performance indicators including IGD-NS, a set of reference points sampled along the Pareto front are required. However, in practice,

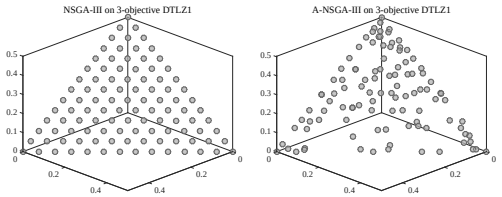

(a) 3-objective DTLZ1

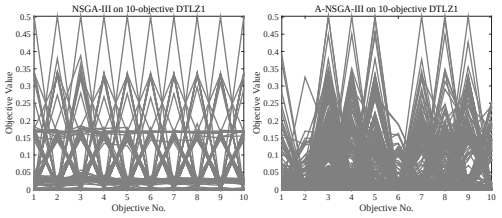

(b) 10-objective DTLZ1

Fig. 1. Final populations obtained by NSGA-III and A-NSGA-III on DTLZ1 with 3 and 10 objectives.

since the true Pareto front is not known *a priori*, a set of reference points are sampled on the basis of the approximate Pareto front obtained by the MOEAs instead. Correspondingly, some reference point adaptation methods have been recently developed to adjust distribution of the reference points to be as similar to the approximate Pareto front as possible [13], [41]–[45]. These reference point adaptation methods can be roughly grouped into two categories. It is worth noting that reference point is also termed as reference vector or weight vector in some decomposition based MOEAs, and in this work, we use the term of reference point as a substitution to others for simplicity.

The first category of methods adjusts the reference points according to the distribution of candidate solutions in the current population at each generation. Two representative methods belonging to this category were proposed in NSGA-III [43] and REVA [13], where the authors named the algorithms with reference point adaptation as A-NSGA-III and RVEA*. In A-NSGA-III, the adaptation method consists of two operations: 1) deleting each added reference point with an empty niche, and 2) randomly adding new reference points inside each crowded reference point with a high niche count. In RVEA* [13], there are two sets of reference vectors, one of which remains uniformly distributed and the other one is adaptively adjusted. The reference vector adaptation also consists of two operations: 1) deleting each reference vector that specifies an empty subspace, and 2) randomly adding new reference vectors inside the hyperbox specified by the nadir point and the ideal point of the current population.

The second category of methods adjusts the reference points according to the distribution of candidate solutions stored in an external archive. Two representative methods along this line were developed in $pa\lambda$-MOEA/D [45] and MOEA/D-AWA [41], respectively. In $pa\lambda$-MOEA/D [45], the area of non-dominated solutions

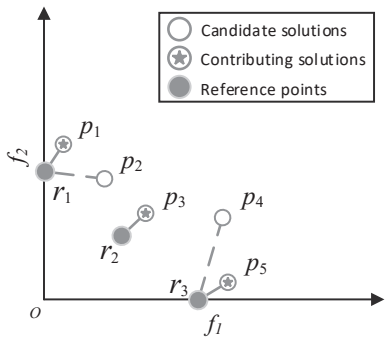

Fig. 2. An illustrative example to show the advantage of IGD-NS indicator over traditional IGD indicator. In the example, the best solution set $\{p_1, p_2, p_3, p_5\}$ can be distinguished by IGD-NS values. By contrast, the traditional IGD indicator is not able to determine such a solution set, since the solution sets $\{p_1, p_3, p_5\}$, $\{p_1, p_2, p_3, p_5\}$, $\{p_1, p_3, p_4, p_5\}$ and $\{p_1, p_2, p_3, p_4, p_5\}$ all have the same IGD value due to the two non-contributing solutions p_2 and p_4.

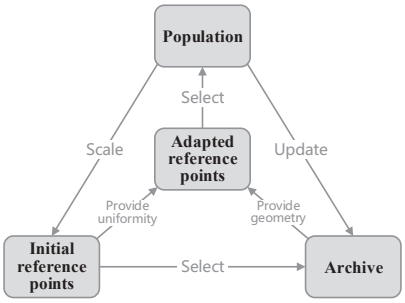

Fig. 3. The relationships between the four sets in AR-MOEA, i.e. the population P, the initial reference point set R, the archive A and the adapted reference point set R'. First, the points in R are scaled according to the range of the non-dominated solutions in P, and the new candidate solutions in P are copied to A. Then, A is truncated based on the points in R. Afterwards, R' is created on the basis of both R and A, where R provides a uniform distribution and A describes the geometry of the Pareto front. Finally, P is truncated (i.e., selection is performed) according to the IGD-NS values calculated with respect to R'.

in the archive is first calculated to estimate the parameter p of Pareto front $f_1^p + \ldots + f_M^p = 1$, where M is the number of objectives. Then, the intersection points between the gradient lines of $\lambda_1 + \ldots + \lambda_M = 1$ and the front are automatically adjusted until a maximum value of hypervolume metric for these points is reached. The intersection points with the maximum hypervolume value are used as the reference points at each generation [45]. In MOEA/D-AWA [41], an archive is used to provide a guidance of adding and removing reference points for better population diversity. If a non-dominated solution in the archive is located in a region having sparse candidate solutions, then this solution is added into the archive and a new reference point will be generated correspondingly; otherwise, the reference point associated with the solution will be deleted.

Despite that most existing reference point adaptation methods have achieved significantly better performance on MOPs with irregular Pareto fronts [13], [41], [43], [45], on the contrary, their performance will considerably deteriorate when applied to MOPs with regular Pareto fronts. To exemplify, Fig. 1 depicts the finial populations obtained by NSGA-III and A-NSGA-III on DTLZ1 with 3 objectives and 10 objectives. It can be clearly observed that the reference point adaptation based A-NSGA-III [43] achieves a worse distribution than the original version with fixed reference point set. This is due to the fact that, although uniformly distributed reference points provide the best approximation to regular Pareto fronts, the adaptation method still perturbs the uniform distribution of the initial reference set. Therefore, the motivation of this work is to propose an MOEA with better versatility on problems with different Pareto fronts, such that it can be applied to the robust optimization of MOPs and MaOPs with various Pareto fronts.

III. The Proposed Algorithm

A. A Brief Summary of IGD-NS

The IGD-NS indicator was developed to distinguish the non-dominated solutions which did not have any contribution in the calculation of IGD [27]. Let X be a set of non-dominated solutions found by an MOEA and Y be a set of reference points, a non-contributing solution $x' \in X$ in the calculation of IGD can be mathematically formulated as

$$\nexists y \in Y \text{ satisfying } dis(y, x') = \min_{x \in X} dis(y, x), \qquad (2)$$

where $dis(y, x)$ denotes the Euclidean distance between y and x in objective space. With the definition of non-contributing solutions, the IGD-NS is defined as

$$\text{IGD-NS}(X, Y) = \sum_{y \in Y} \min_{x \in X} dis(y, x) + \sum_{x' \in X^*} \min_{y \in Y} dis(y, x'), \qquad (3)$$

where X^* denotes the non-contributing solution set in X [27].

Compared to the traditional IGD indicator, IGD-NS provides a more comprehensive evaluation of a given solution set. Let us consider an example as shown in Fig. 2, where p_1, p_3 and p_5 are contributing solutions, and p_2 and p_4 are non-contributing solutions. In the case that four out of the five candidate solutions need to be selected for next generation, the IGD-NS indicator is able to assign the minimum value to $\{p_1, p_2, p_3, p_5\}$, which are the best candidate solutions in terms of convergence and diversity. By contrast, for the traditional IGD, it is impossible to distinguish these four candidate solutions as both p_2 and p_4 are non-contributing solutions, such that the solution set $\{p_1, p_3, p_5\}$ has the same IGD value with $\{p_1, p_2, p_3, p_5\}$, $\{p_1, p_3, p_4, p_5\}$ and $\{p_1, p_2, p_3, p_4, p_5\}$.

B. A General Framework of AR-MOEA

The proposed AR-MOEA has a similar framework as most existing indicator based MOEAs, except that IGD-NS is adopted as the indicator and a reference point

Algorithm 1: General Framework of AR-MOEA

Input: N (population size), N_R (number of reference points and archive size)
Output: P (final population)

$P \leftarrow RandomInitialize(N)$;
$R \leftarrow UniformReferencePoint(N_R)$;
$A \leftarrow P$;
$R' \leftarrow R$;
while *termination criterion not fulfilled* **do**
  $P' \leftarrow MatingSelection(P, R')$;
  $O \leftarrow Variation(P', N)$;
  $[A, R'] \leftarrow RefPointAdaption(A \cup O,\ R, P)$;
  $P \leftarrow EnvironmentalSelection(P \cup O, R', N)$;
return P;

Algorithm 2: $MatingSelection(P, R')$

Input: P (population), R' (set of adapted reference points)
Output: P' (parents for variation)

for $i = 1$ *to* M **do**
  /*M denotes the number of objectives*/
  $f_i(p) \leftarrow f_i(p) - \min_{q \in P} f_i(q), \forall p \in P$;
Calculate the fitness of each solution by Equation (4);
$P' \leftarrow \emptyset$;
for $i = 1$ *to* $|P|$ **do**
  Randomly select p and q from P;
  if $fitness_p > fitness_q$ **then**
    $P' \leftarrow P' \cup \{p\}$;
  else
    $P' \leftarrow P' \cup \{q\}$;
return P';

adaptation method is developed for the calculation of IGD-NS at each generation. In general, there are four main solution sets maintained in AR-MOEA, i.e. the population P, the initial reference point set R, the archive A and the adapted reference point set R'. To be specific, the population P contains the candidate solutions as final output, the initial reference point set R is used to guarantee uniform distribution of the candidate solutions in P, the archive A reflects the Pareto front and guides the reference point adaptation, and the adapted reference point set R' is used in the IGD-NS based selection for truncating the population P, where the relationships between the four solution sets are described in Fig. 3.

As presented in Algorithm 1, the main framework of AR-MOEA consists of the following steps. First, an initial population P of size N is randomly generated, and a set of uniformly distributed reference points R of size N_R is predefined. Then, in the main loop, a binary tournament strategy is employed to create a mating pool P' of size N according to the contribution $fitness_p$ of each candidate

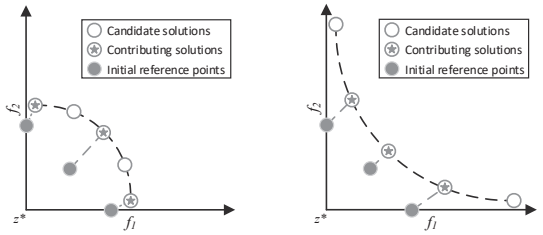

(a) Solutions lie on a concave surface

(b) Solutions lie on a convex surface

Fig. 4. The contributing solutions in a solution set lying on a concave and convex surface respectively.

solution p to the population P in terms of the IGD-NS value:

$$fitness_p = \text{IGD-NS}(P \backslash \{p\}, R'), \tag{4}$$

where R' is a set of reference points for calculating IGD-NS. Algorithm 2 details the procedure of IGD-NS based mating selection strategy in AR-MOEA. To be specific, for any two solutions randomly picked from the parent population P, the one with a larger contribution to the IGD-NS value of P will be the winner, and vice versa. After N offspring individuals are created based on the mating pool P', the proposed reference point adaptation method is employed to adjust the reference points and the archive A. Finally, the IGD-NS based environmental selection is performed to select N candidate solutions from the combined population. The above steps will repeat until a termination criterion is reached.

In the next two subsections, we will further detail the two main components of the proposed AR-MOEA, namely, the reference point adaptation method and the IGD-NS based environmental selection, respectively.

C. A Reference Point Adaptation Method

Algorithm 3 presents the procedure of the proposed reference point adaptation method, which consists of the following three operations: 1) normalizing archive A, population P and reference point set R, 2) updating archive A, and 3) adapting reference point set R. To begin with, the ideal point z_i^* and nadir point z_i^{nad} of the current population P are adaptively estimated using the objective vectors in the current population. Then, the values on each objective i of the solutions in archive A and population P are translated by subtracting z_i^*, and the values on each objective i of the reference points in R are scaled by multiplying $z_i^{nad} - z_i^*$. As reported in [13], with the above transformations, all the values in A, P and R will be normalized into the same region $\prod_{i=1}^{M}[0, z_i^{nad} - z_i^*]$, such that uniformly distributed reference points can produce uniformly distributed solutions regardless of the scales of different objectives.

After A, P and R are normalized into the same range, archive A will be updated by the second operation in Algorithm 3. During the updating procedure, first, all redundant or dominated solutions in A are deleted.

Algorithm 3: $RefPointAdaption(A, R, P)$

Input: A (original archive), R (set of initial reference points), P (population)
Output: A' (new archive), R' (set of adapted reference points)

/*Operation 1: translate A, P and scale R*/
for $i = 1$ *to* M **do**
  /*M denotes the number of objectives*/
  $z_i^* \leftarrow \min_{p \in P} f_i(p)$;
  $z_i^{nad} \leftarrow \max_{p \in P} f_i(p)$;
  $f_i(p) \leftarrow f_i(p) - z_i^*, \forall p \in A \cup P$;
  $R_i^j \leftarrow R_i^j * (z_i^{nad} - z_i^*), \forall j \in \{1, \ldots, |R|\}$;
  /*R_i^j is the i-th value of the j-th point in R*/
/*Operation 2: update archive*/
Delete duplicate candidate solutions in A;
Delete dominated candidate solutions in A;
$R \leftarrow AdjustLocation(R, A)$;
$A^{con} \leftarrow \{p \in A | \exists r \in R : dis(r, F(p)) = \min_{q \in A} dis(r, F(q))\}$;
$A' \leftarrow A^{con}$;
while $|A'| < \min(|R|, |A|)$ **do**
  $p \leftarrow \text{argmax}_{p \in A \setminus A'} \min_{q \in A'} \arccos(F(p), F(q))$;
  $A' \leftarrow A' \cup \{p\}$;
/*Operation 3: adapt reference points*/
$R^{valid} \leftarrow \{r \in R | \exists p \in A^{con} : dis(r, F(p)) = \min_{s \in R} dis(s, F(p))\}$;
$R' \leftarrow R^{valid}$;
while $|R'| < \min(|R|, |A'|)$ **do**
  $p \leftarrow \text{argmax}_{p \in A' \setminus R'} \min_{r \in R'} \arccos(r, F(p))$;
  $R' \leftarrow R' \cup \{F(p)\}$;
$R' \leftarrow AdjustLocation(R', P)$;
return A' and R';

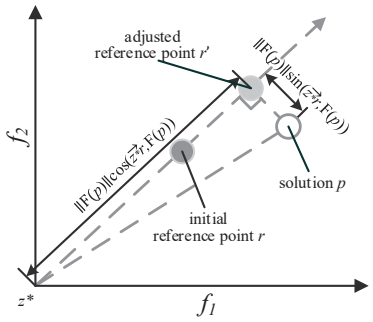

Fig. 5. Illustration of location adjustment of reference point r according to solution p.

Then, the contributing solutions in A are detected and copied to A^{con}, where the "contributing solutions" are those closest to at least one point in R according to the definition of IGD-NS. As an example, Fig. 4 shows two archives containing five solutions which lie on a concave surface and a convex surface, respectively, where the three solutions close to the three reference points in each archive are regarded as contributing solutions. It is worth

Algorithm 4: $AdjustLocation(R, P)$

Input: R (set of reference points), P (population)
Output: R' (set of adjusted reference points)

$R' \leftarrow \emptyset$;
forall the $r \in R$ **do**
  $p \leftarrow \text{argmin}_{p \in P} \|F(p)\| \sin(\overrightarrow{z^*r}, F(p))$;
  $r'_i \leftarrow r_i / \|r\| * \|F(p)\| \cos(\overrightarrow{z^*r}, F(p)), \forall i \in \{1, \ldots, M\}$;
  $R' \leftarrow R' \cup \{r'\}$;
return R';

noting that as shown in Fig. 4 (b), the two extreme solutions cannot be treated as contributing solutions when they lie on a convex surface, such that the contributing solutions can only locate in the middle region of the whole space in the objective space. In order to preserve extreme solutions for better diversity, we adjust the location of each reference point before the contribution solution detection is performed, where the adjusting approach is illustrated in Fig. 5. To be specific, for each reference point r, the solution p having the minimum perpendicular distance to vector $\overrightarrow{z^*r}$ is detected, then the location of r is changed to the orthogonal projection of $F(p)$ on vector $\overrightarrow{z^*r}$, where z^* is the ideal point. The pseudocode of location adjustment of each reference point is given in Algorithm 4. After the adjustment of reference points and the detection of contributing solutions are finished, all the contributing solutions are copied from A^{con} to the new archive A', and the remaining space of A' is filled up by candidate solutions from $A \setminus A'$ one by one until A' reaches its maximal size of $\min(|R|, |A|)$, where at each time the candidate solution p having the maximum value of $\min_{q \in A'} \arccos(F(p), F(q))$ in $A \setminus A'$ is copied to A', with $\arccos(F(p), F(q))$ indicating the acute angle between p and q in objective space. In this way, the archive always contains a number of non-dominated solutions with good distribution, and has the same size as the reference point set.

As the third operation of Algorithm 3, the reference point adaptation strategy is performed based on the reference point set R and the new archive A'. To begin with, all reference points closest to the contributing solutions in A^{con} are detected as valid reference points, and then copied to R^{valid}. Afterwards, all the valid reference points in R^{valid} are copied to the set of adapted reference point set R'. Then, the remaining space of R' is filled with candidate solutions from A' one by one until $|R'| = \min(|R|, |A'|)$ is reached, where at each time the solution p having the maximum value of $\min_{r \in R'} \arccos(r, F(p))$ in $A' \setminus R'$ is copied to R'. Finally, since the adapted reference point set R' will be used to perform environmental selection on the current population P, the reference points in R' are also adaptively adjusted using Algorithm 4.

Fig. 6 presents an example to illustrate the above pro-

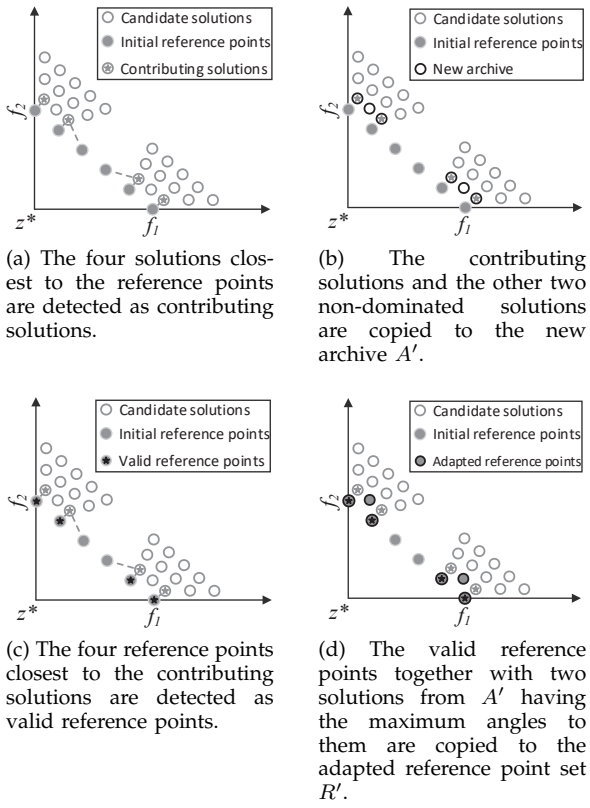

(a) The four solutions closest to the reference points are detected as contributing solutions.

(b) The contributing solutions and the other two non-dominated solutions are copied to the new archive A'.

(c) The four reference points closest to the contributing solutions are detected as valid reference points.

(d) The valid reference points together with two solutions from A' having the maximum angles to them are copied to the adapted reference point set R'.

Fig. 6. Illustration to the procedure of archive update and reference point adaptation.

cedure of archive update and reference point adaptation. First of all, as shown in Fig. 6 (a), the four candidate solutions closest to the six reference points are detected as contributing solutions. Then, as shown in Fig. 6 (b), the four contributing solutions are copied to the new archive A', together with the other two non-dominated solutions having the maximum angles to them. Thirdly, the four reference points closest to the four contributing solutions are detected as valid reference points as shown in Fig. 6 (c). And finally as shown in Fig. 6 (d), the four valid reference points and two candidate solutions from A' having the maximum angles to them are copied to the adapted reference point set R'.

Therefore, the adapted reference point set R' consists of the valid reference points from R and the candidate solutions from A', where R' is able to not only maintain a uniform distribution provided by R, but also reflect the shape of the approximate Pareto front stored in A', and the ratios of valid reference points and candidate solutions in R' can be adaptively adjusted. To exemplify, Fig. 7 illustrates the average ratio of valid reference points in R' at different generations on 3-objective DTLZ1 and DTLZ6 over 30 runs. To be specific, since DTLZ1 has a regular Pareto front, all the initial reference points in R are always valid until the final generation; on the contrary, since 3-objective DTLZ6 has a degenerate Pareto front, only a few initial reference points close to the degenerate Pareto front can be detected as valid ones.

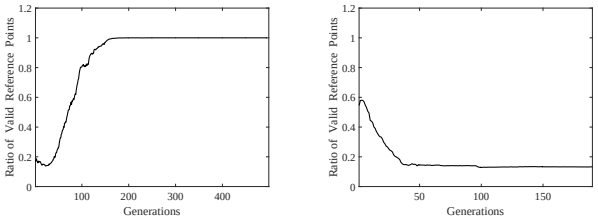

(a) 3-objective DTLZ1 (b) 3-objective DTLZ6

Fig. 7. Average ratio of valid reference points in AR-MOEA at different generations for solving 3-objective DTLZ1 and DTLZ6 over 30 runs, where the total number of reference points is 105.

Algorithm 5: $EnvironmentalSelection(P, R', N)$

Input: P (combined population), R' (set of adapted reference points), N (size of population)
Output: Q (population for next generation)

for $i = 1$ *to* M **do**
  /*M denotes the number of objectives*/
  $f_i(p) \leftarrow f_i(p) - \min_{q \in P} f_i(q), \forall p \in P$;
$Front \leftarrow NondominatedSort(P)$;
$k \leftarrow$ the minimum number satisfies $|\bigcup_{i=1}^{k} Front_i| \geq N$;
$Q \leftarrow \bigcup_{i=1}^{k-1} Front_i$;
while $|Front_k| > N - |Q|$ **do**
  $p \leftarrow \text{argmin}_{p \in Front_k} \text{IGD-NS}(Front_k \backslash \{p\}, R')$;
  $Front_k \leftarrow Front_k \backslash \{p\}$;
$Q \leftarrow Q \cup Front_k$;
return Q;

D. IGD-NS based Environmental Selection

Similar to most existing MOEAs, the AR-MOEA also adopts the elite strategy by performing the environmental selection on the combined population of parent and offspring candidate solutions at each generation.

The procedure of the IGD-NS based environmental selection is given in Algorithm 5. Before the IGD-NS indicator is used for candidate solution selection, the combined population is first sorted by the efficient non-dominated sort (ENS) [46] for MOPs and tree-based ENS (T-ENS) [47] for MaOPs. Then, all the candidate solutions in the first $k-1$ fronts are directly selected for next generation, and the IGD-NS indicator is used to select solutions in the k-th front $Front_k$, where k denotes the minimum number satisfying $|\bigcup_{i=1}^{k} Front_i| \geq N$. For each solution in $Front_k$, its contribution to $Front_k$ on IGD-NS is calculated according to Formula (4), and the solution having the least contribution will be deleted from $Front_k$. Each time after a candidate solution is deleted, the contribution of each remaining solution in $Front_k$ is recalculated, and this process is repeated until the number of remaining solutions in $\bigcup_{i=1}^{k} Front_i$ reaches N.

It is worth noting that, although the selection process in most decomposition based MOEAs is also guided

TABLE I
SETTINGS OF THE NUMBER OF OBJECTIVES, THE NUMBER OF DECISION VARIABLES AND THE MAXIMAL NUMBER OF GENERATIONS FOR EACH TEST PROBLEM.

Problem	No. of objectives (M)	No. of variables (D)	No. of generations (G_{max})	Pareto front
Regular Pareto front				
DTLZ1	3,5,10	M-1+5	500	Linear
DTLZ2,4	3,5,10	M-1+10	200	Concave
DTLZ3	3,5,10	M-1+10	500	Concave
WFG4–9	3,5,10	M-1+10	200	Concave
Pareto-Box	3,5,10	2	500	Concave
Irregular Pareto front				
DTLZ5–6	3,5,10	M-1+10	200	Mostly degenerate
DTLZ7	3,5,10	M-1+20	200	Disconnected
IDTLZ1	3,5,10	M-1+5	500	Inverted
IDTLZ2	3,5,10	M-1+10	200	Inverted
WFG1	3,5,10	M-1+10	500	Sharp tails
WFG2	3,5,10	M-1+10	500	Disconnected
WFG3	3,5,10	M-1+10	200	Mostly degenerate
MaF2	3,5,10	M-1+10	500	Disconnected
MaF4	3,5,10	M-1+10	500	Inverted
MaF13	3,5,10	5	500	Degenerate

* The Pareto fronts of DTLZ5 and DTLZ6 with four or more objectives are not degenerate [50]–[52]. The Pareto front of WFG3 is also not completely degenerate [52].

by a set of reference/weight vectors, the motivation of employing reference points in AR-MOEA is completely different. In AR-MOEA, the reference points are merely used as reference for the calculation of IGD-NS, while in decomposition based MOEAs, each candidate solution is associated with one reference point. Since there does not exist any association between candidate solutions and reference points, the population size of AR-MOEA can be an arbitrary number smaller than the number of reference points, not necessarily being identical to the requirements of sampling method such as Das and Dennis's systematic approach [48] and the approach proposed by He *et al.* [49]. This conclusion will be further supported by the empirical results in Section IV-D, regardless of specific population size, AR-MOEA is always able to obtain a set of uniformly distributed candidate solutions, which is a major advantage over existing MOEAs using predefined reference points.

IV. EXPERIMENTAL RESULTS AND ANALYSIS

In this section, we first compare the proposed AR-MOEA with four MOEAs designed for solving MOPs, namely, MOEA/D [12], NSGA-II [3], PESA-II [5] and IBEA [18], and four MOEAs for handling MaOPs, namely, MOEA/DD [53], NSGA-III [16], RVEA [13] and MOMBI-II [21]. Then, the effectiveness of the reference point adaptation method in AR-MOEA is assessed via comparisons with two state-of-the-art reference point adaptation methods, namely, those in A-NSGA-III [43] and RVEA* [13]. Finally, sensitivity analysis on population size in the proposed AR-MOEA is performed.

TABLE II
SETTINGS OF NUMBER OF REFERENCE POINTS FOR EACH NUMBER OF OBJECTIVES, WHERE p_1 AND p_2 DENOTE THE NUMBERS OF DIVISIONS ON EACH OBJECTIVE FOR THE BOUNDARY LAYER AND THE INSIDER LAYER, RESPECTIVELY.

Number of objectives (M)	Parameter (p_1, p_2)	Number of reference points/ Population size (N)
3	13, 0	105
5	5, 0	126
10	3, 2	275

Among the compared algorithms, MOEA/D, NSGA-II, PESA-II and IBEA are four classical MOEAs for solving MOPs, where MOEA/D is a decomposition based MOEA, NSGA-II and PESA-II are Pareto dominance based MOEAs and IBEA is an indicator based MOEA; MOEA/DD, NSGA-III and RVEA are three popular decomposition based MOEAs, which have shown competitive performance on both MOPs and MaOPs with regular Pareto fronts; and MOMBI-II is a recently proposed indicator based MOEA, where a set of uniformly distributed reference points are used in the calculation of R2 indicator. In addition, A-NSGA-III and RVEA* are modified versions of NSGA-III and RVEA with reference point adaptation methods, which were suggested to handle problems with irregular Pareto fronts.

In the experiments, 22 test problems from five widely used test suites are employed in total, namely DTLZ1–DTLZ7 [54], IDTLZ1, IDTLZ2 [43], WFG1–WFG9 [50], MaF2, MaF4, MaF13 [55] and Pareto-Box problem [56], where the relevant settings are given in Table I. DTLZ1–DTLZ7 and WFG1–WFG9 are problems with scalable number of objectives, which are widely used to test the performance of MOEAs on MOPs and MaOPs. IDTLZ1 and IDTLZ2 denote the problems of inverted DTLZ1 and DTLZ2, respectively, where the regular Pareto fronts of DTLZ1 and DTLZ2 are inverted and thus become irregular [26]. The MaF test suite is designed for the CEC 2017 competition on evolutionary many-objective optimization, where MaF2, MaF4 and MaF13 are with highly irregular Pareto fronts. The Pareto-Box problem, which also has a scalable number of objectives, is usually used to provide a visual and intuitive assessment of MOEAs in many-objective optimization. Among the test problems considered in the paper, DTLZ5–DTLZ7, IDTLZ1, IDTLZ2, WFG1–WFG3, MaF2, MaF4 and MaF13 are with irregular Pareto fronts, and the others are with regular Pareto fronts.

A. Experimental Settings

1) Reference points: The uniformly distributed reference points generated by Das and Dennis's approach with two layers [16] are adopted in MOEA/D, MOEA/DD, NSGA-III, RVEA and MOMBI-II. Table II lists the number of reference points used in the experiments for each number of objectives, where p_1 and p_2 denote the

TABLE III
IGD VALUES OBTAINED BY MOEA/D, NSGA-II, PESA-II, IBEA AND AR-MOEA ON DTLZ1–DTLZ7, IDTLZ1, IDTLZ2, WFG1–WFG9 AND PARETO-BOX PROBLEM WITH 3 OBJECTIVES. THE BEST RESULT IN EACH ROW IS HIGHLIGHTED.

Problem	Obj.	MOEA/D	NSGA-II	PESA-II	IBEA	AR-MOEA	Pareto front
DTLZ1	3	1.8973e-2(3.89e-5)≈	2.6772e-2(1.36e-3)−	2.4569e-2(1.83e-3)−	1.5614e-1(2.52e-2)−	1.8972e-2(3.52e-5)	Regular
DTLZ2		5.1303e-2(4.38e-4)−	6.7599e-2(2.65e-3)−	6.5089e-2(4.28e-3)−	7.8499e-2(2.34e-3)−	5.0244e-2(6.34e-5)	
DTLZ3		5.4281e-2(2.52e-3)−	1.0247e-1(1.73e-1)−	7.3562e-2(8.90e-3)−	4.7661e-1(6.55e-3)−	5.2839e-2(1.67e-3)	
DTLZ4		4.1204e-1(3.65e-1)−	1.2481e-1(2.23e-1)+	9.2065e-2(1.61e-1)+	7.8047e-2(2.41e-3)+	1.6466e-1(2.11e-1)	
WFG4	3	2.3666e-1(4.52e-3)−	2.6626e-1(9.40e-3)−	2.8126e-1(1.28e-2)−	3.1204e-1(1.24e-2)−	2.0545e-1(9.68e-4)	
WFG5		2.3362e-1(3.25e-3)−	2.7357e-1(8.15e-3)−	2.7872e-1(1.17e-2)−	3.1754e-1(1.49e-2)−	2.1455e-1(4.35e-4)	
WFG6		2.7702e-1(1.65e-2)−	3.1256e-1(1.58e-2)−	3.2250e-1(2.16e-2)−	3.2584e-1(1.70e-2)−	2.3011e-1(1.02e-2)	
WFG7		2.9086e-1(2.47e-2)−	2.7558e-1(8.75e-3)−	2.8244e-1(1.84e-2)−	3.1522e-1(1.19e-2)−	2.0709e-1(8.27e-4)	
WFG8		3.1027e-1(1.12e-2)−	3.6237e-1(1.18e-2)−	3.7464e-1(1.57e-2)−	3.3821e-1(9.29e-3)−	2.8153e-1(2.22e-3)	
WFG9		2.9796e-1(5.59e-2)−	2.7857e-1(2.35e-2)−	2.7259e-1(2.39e-2)−	2.8865e-1(1.21e-2)−	2.0875e-1(2.24e-3)	
Pareto-Box	3	3.8995e+0(3.81e-3)−	3.3723e+0(1.78e-1)−	2.9850e+0(7.24e-2)−	2.7430e+0(4.80e-2)+	2.8679e+0(4.39e-2)	
+/ − / ≈		0/10/1	1/10/0	1/10/0	2/9/0		
DTLZ5	3	3.0912e-2(1.93e-4)−	5.4299e-3(2.61e-4)−	1.1310e-2(1.43e-3)−	1.5396e-2(1.75e-3)−	4.6091e-3(1.09e-4)	Irregular
DTLZ6		3.0938e-2(4.47e-4)−	4.9648e-3(2.09e-4)−	1.0987e-2(1.55e-3)−	2.6810e-2(4.13e-3)−	4.2651e-3(6.62e-5)	
DTLZ7		1.2746e-1(1.48e-3)−	7.4897e-2(3.32e-3)−	1.3555e-1(1.22e-1)−	1.0429e-1(1.43e-1)−	6.2010e-2(9.20e-4)	
IDTLZ1		3.0679e-2(1.48e-4)−	2.6913e-2(1.36e-3)−	2.3576e-2(1.36e-3)−	2.4184e-1(1.02e-2)−	2.0530e-2(1.39e-4)	
IDTLZ2		5.8735e-2(2.24e-4)−	6.8555e-2(2.61e-3)−	6.0290e-2(1.26e-3)−	6.3748e-2(2.08e-3)−	5.7133e-2(3.89e-4)	
WFG1	3	3.6315e-1(3.72e-2)−	2.5333e-1(3.02e-2)−	2.3729e-1(4.04e-2)−	2.0751e-1(1.18e-2)−	1.5906e-1(1.17e-2)	
WFG2		9.5329e-1(7.30e-2)−	1.9063e-1(1.27e-2)−	1.9380e-1(1.23e-2)−	2.5207e-1(5.45e-3)−	1.7238e-1(4.52e-3)	
WFG3		2.2093e-1(8.31e-2)−	1.0222e-1(1.77e-2)+	4.1376e-1(2.30e-1)−	3.7973e-2(2.03e-3)+	1.2689e-1(6.61e-3)	
MaF2	3	3.7797e-2(1.07e-3)−	4.6569e-2(1.76e-3)−	3.2747e-2(1.10e-3)−	3.1905e-2(6.53e-4)−	2.9902e-2(5.78e-4)	
MaF4		8.2102e-1(1.13e-1)−	3.0051e-1(1.16e-2)+	2.9740e-1(2.25e-2)+	6.9339e-1(9.35e-2)−	3.1239e-1(7.05e-3)	
MaF13		9.4029e-2(8.59e-3)−	1.0941e-1(8.38e-3)−	1.8657e-1(9.69e-2)−	4.4711e-1(4.72e-2)−	7.7328e-2(4.89e-3)	
+/ − / ≈		0/11/0	2/9/0	1/10/0	1/10/0		

'+', '−' and '≈' indicate that the result is significantly better, significantly worse and statistically similar to that obtained by AR-MOEA, respectively.

numbers of divisions on each objective for the boundary layer and the insider layer, respectively. For fair comparisons, the proposed AR-MOEA also adopts the same predefined reference points as listed in Table II, and the population size for each compared MOEA is set to the same as the number of reference points.

2) Parameters in the compared MOEAs: For PESA-II, the number of divisions in each objective is set to 10. For IBEA, the fitness scaling factor κ is set to 0.05. For MOEA/D and MOEA/DD, the size of neighborhood T is set to $\lceil 0.1 \times N \rceil$ (with N denoting the population size), and the neighborhood selection probability δ is set to 0.9. In addition, for MOEA/D, the maximum number of solutions replaced by each offspring n_r is set to $\lceil 0.01 \times N \rceil$, and the Tchebycheff approach (with transformed reference points [57]) is employed as the aggregation function. For RVEA and RVEA*, the penalty parameter α is set to 2, and the frequency of reference point adaption f_r is set to 0.1. For MOMBI-II, the threshold of variance α, the tolerance threshold ϵ and the *record* size of nadir vectors are set to 0.5, 0.001 and 5, respectively. For NSGA-II, NSGA-III, A-NSGA-III and AR-MOEA, however, there is no additional parameter to be specified.

3) Genetic operators: The simulated binary crossover (SBX) [58] and polynomial mutation [59] are applied in all MOEAs. The probabilities of crossover and mutation are set to 1.0 and $1/D$ (with D denoting the number of decision variables). The distribution indexes of both SBX and polynomial mutation are set to 20.

4) Performance metrics: The inverted generational distance (IGD) [29] and the hypervolume (HV) [30] are adopted to measure the solution sets in terms of both convergence and diversity quality. All the objective values are normalized by the ideal point and nadir point of the Pareto optimal front before HV calculation, then the normalized HV value of the solution set is calculated with a reference point $(1.1, 1.1, \ldots, 1.1)$. Besides, the Monte Carlo estimation method with 1,000,000 sampling points is adopted for problems with ten objectives for higher computational efficiency. In the calculation of IGD, roughly 5,000 uniformly distributed points are sampled on the Pareto front by Das and Dennis's approach for each test instance. All the tests are run for 30 times independently, and the mean and standard deviation of each metric value are recorded. The Wilcoxon rank sum test with a significance level of 0.05 is adopted to perform statistical analysis on the experimental results, where the symbols '+', '−' and '≈' indicate that the result by another MOEA is significantly better, significantly worse and statistically similar to that obtained by AR-MOEA, respectively.

B. Comparisons between AR-MOEA and Existing MOEAs for Solving MOPs and MaOPs

Table III presents the IGD values obtained by AR-MOEA and four popular MOEAs designed for solving MOPs, namely, MOEA/D, NSGA-II, PESA-II and IBEA on DTLZ1–DTLZ7, IDTLZ1, IDTLZ2, WFG1–WFG9, MaF2, MaF4, MaF13 and the Pareto-Box prob-

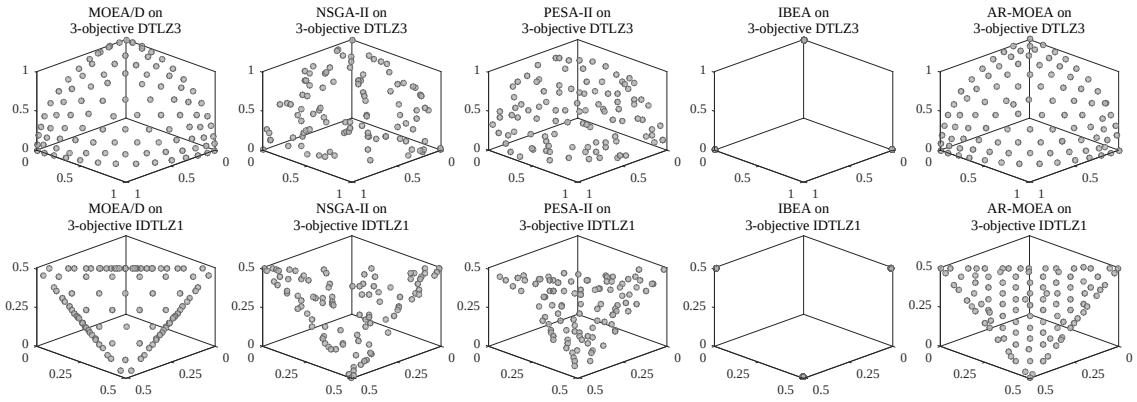

Fig. 8. The non-dominated solution set with the median IGD value among 30 runs obtained by MOEA/D, NSGA-II, PESA-II, IBEA and AR-MOEA on DTLZ3 and IDTLZ1 with 3 objectives.

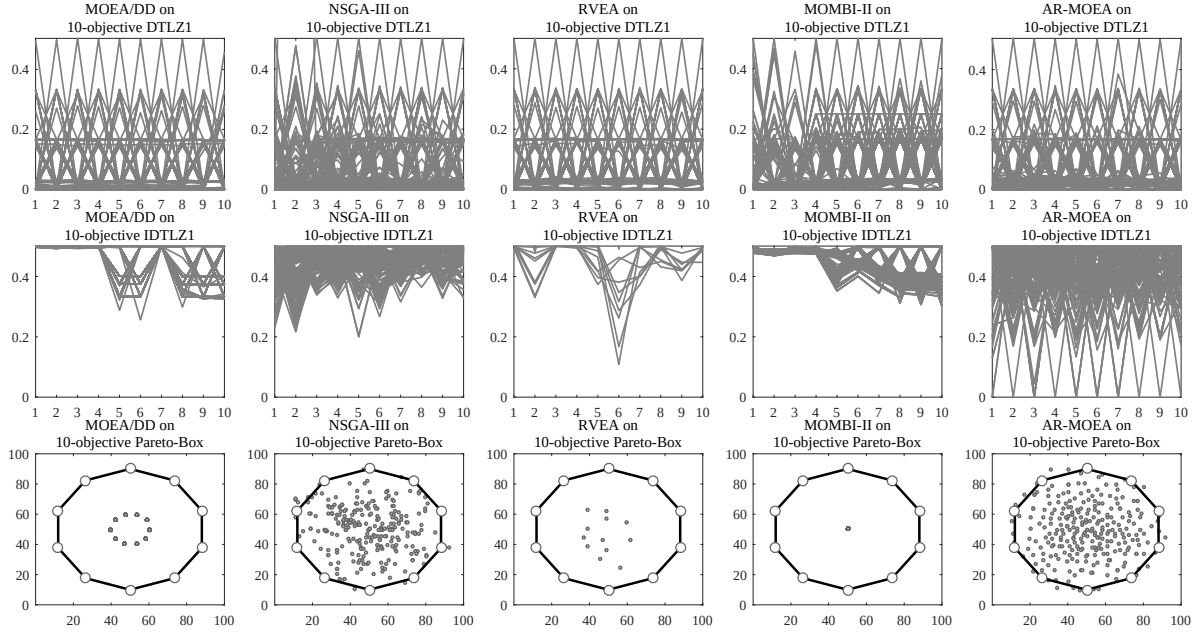

Fig. 9. The parallel coordinates of the objective values of the non-dominated solution set on 10-objective DTLZ1 and IDTLZ1 and the decision variables of the non-dominated solution set on 10-objective Pareto-Box problem, obtained by MOEA/DD, NSGA-III, RVEA, MOMBI-II and AR-MOEA with the median HV value among 30 runs.

lem with three objectives. In general, the proposed AR-MOEA significantly outperforms the other four MOEAs in terms of the IGD values, having achieved the best performance on 9 of 11 instances with regular Pareto fronts and all the instances with irregular Pareto fronts except for WFG3 and MaF4. As can be further observed from Fig. 8, the solution sets obtained by AR-MOEA have shown uniform distributions on both DTLZ3 and IDTLZ1. To be specific, for instances with a regular Pareto front such as DTLZ3, the uniformly distributed reference points in the initial reference set will not be updated by the candidate solutions in the archive as all the initial reference points are detected as valid ones, thus providing a uniform coverage of the regular Pareto front; by contrast, for instances with an irregular Pareto front such as IDTLZ1, the distribution of the reference points will be adaptively adjusted according to the shape of the approximate Pareto front stored in the archive. Therefore, as evidenced by Table III and Fig. 8, AR-MOEA has promising versatility in the optimization of MOPs with various Pareto fronts.

Table IV presents the HV values obtained by AR-MOEA and four state-of-the-art MOEAs designed for solving MaOPs, namely, MOEA/DD, NSGA-III, RVEA and MOMBI-II on DTLZ1–DTLZ7, IDTLZ1, IDTLZ2, WFG1–WFG9, MaF2, MaF4, MaF13 and the Pareto-Box problem with 5 and 10 objectives. In general, AR-MOEA has achieved the best performance on 23 of 44 instances, while the number of best results obtained by MOEA/DD, NSGA-III, RVEA and MOMBI-II are 3, 7, 6 and 5, respectively. On one hand, the performance of AR-MOEA is comparable to RVEA on MaOPs with regular Pareto fronts; on the other hand, AR-MOEA performs much better than the four compared algorithms on

TABLE IV
HV VALUES OBTAINED BY MOEA/DD, NSGA-III, RVEA, MOMBI-II AND AR-MOEA ON DTLZ1–DTLZ7, IDTLZ1, IDTLZ2, WFG1–WFG9 AND PARETO-BOX PROBLEM WITH 5, 8 AND 10 OBJECTIVES. THE BEST RESULT IN EACH ROW IS HIGHLIGHTED.

Problem	Obj.	MOEA/DD	NSGA-III	RVEA	MOMBI-II	AR-MOEA	Pareto front
DTLZ1	5	9.7487e-1(1.94e-4)≈	9.7456e-1(4.86e-4)−	9.7478e-1(3.14e-4)−	9.7351e-1(4.42e-3)−	9.7492e-1(1.53e-4)	Regular
	10	9.9957e-1(4.55e-5)−	9.8390e-1(4.66e-2)−	9.9967e-1(2.82e-5)−	9.6925e-1(2.65e-2)−	9.9971e-1(8.84e-6)	
DTLZ2	5	7.9294e-1(5.49e-2)+	7.9035e-1(8.70e-4)≈	7.9209e-1(6.51e-4)+	7.9047e-1(8.76e-4)≈	7.9047e-1(8.44e-4)	
	10	9.6735e-1(2.41e-4)+	9.4923e-1(3.10e-2)−	9.6751e-1(2.27e-4)+	9.6676e-1(1.15e-3)+	9.6432e-1(8.26e-4)	
DTLZ3	5	7.7880e-1(1.20e-2)+	5.9177e-1(2.97e-1)−	7.3843e-1(7.61e-2)−	7.8044e-1(6.59e-3)+	7.7241e-1(7.36e-3)	
	10	9.6669e-1(2.00e-3)≈	3.8532e-1(3.38e-1)−	9.6065e-1(6.15e-3)−	8.9039e-1(8.97e-2)−	9.6723e-1(2.93e-3)	
DTLZ4	5	7.9366e-1(5.01e-4)+	7.8203e-1(2.89e-2)−	7.9307e-1(4.99e-4)+	7.8440e-1(2.23e-2)−	7.9077e-1(6.88e-4)	
	10	9.6837e-1(3.23e-3)≈	9.6625e-1(9.90e-4)−	9.6964e-1(2.83e-4)+	9.7283e-1(2.42e-3)+	9.6902e-1(5.57e-4)	
WFG4	5	7.3376e-1(4.22e-3)−	7.5449e-1(3.69e-3)≈	7.5308e-1(4.07e-3)≈	6.6398e-1(5.23e-2)−	7.5453e-1(2.07e-3)	
	10	7.6743e-1(1.93e-2)−	8.9857e-1(5.60e-3)+	8.8241e-1(1.01e-2)−	8.7462e-1(5.84e-2)≈	8.8966e-1(4.85e-3)	
WFG5	5	7.0007e-1(3.02e-3)−	7.2681e-1(2.69e-3)+	7.3480e-1(3.06e-3)+	6.5742e-1(2.62e-2)−	7.2382e-1(3.37e-3)	
	10	7.0849e-1(1.66e-2)−	8.6801e-1(3.68e-3)+	8.8266e-1(3.17e-3)+	7.9516e-1(8.77e-3)−	8.6084e-1(3.65e-3)	
WFG6	5	6.7509e-1(2.06e-2)−	6.9299e-1(1.74e-2)−	6.9327e-1(1.77e-2)−	5.9610e-1(7.47e-2)−	7.0243e-1(1.35e-2)	
	10	7.0328e-1(2.19e-2)−	8.3663e-1(1.99e-2)−	8.4231e-1(1.84e-2)≈	7.7700e-1(2.03e-2)−	8.4757e-1(1.87e-2)	
WFG7	5	7.3417e-1(7.96e-3)−	7.6421e-1(3.10e-3)+	7.8038e-1(1.45e-3)+	7.1239e-1(5.18e-2)−	7.5296e-1(5.22e-3)	
	10	8.2374e-1(1.73e-2)−	9.1967e-1(7.35e-3)+	9.2839e-1(3.85e-3)+	8.9363e-1(7.26e-3)−	9.0021e-1(7.43e-3)	
WFG8	5	6.2760e-1(1.43e-2)−	6.3989e-1(5.93e-3)−	6.3164e-1(8.58e-3)−	3.1383e-1(6.14e-3)−	6.5054e-1(3.62e-3)	
	10	6.3576e-1(6.52e-2)−	7.8406e-1(1.67e-2)−	6.9757e-1(7.24e-2)−	6.8159e-1(1.27e-2)−	8.1960e-1(8.69e-3)	
WFG9	5	6.4941e-1(2.17e-2)−	6.9920e-1(2.43e-2)+	7.2044e-1(8.42e-3)+	4.2002e-1(5.78e-2)−	6.7695e-1(1.32e-2)	
	10	6.2337e-1(4.30e-2)−	8.3169e-1(2.84e-2)+	8.3135e-1(1.92e-2)+	8.1153e-1(1.40e-2)+	7.9046e-1(2.12e-2)	
Pareto-Box	5	8.5731e-2(2.83e-4)−	1.1440e-1(1.90e-3)−	8.4927e-2(3.17e-3)−	8.8464e-2(6.41e-4)−	1.3000e-1(4.92e-4)	
	10	6.6708e-3(8.62e-4)−	1.2292e-2(1.13e-4)−	6.8322e-3(4.15e-4)−	2.5751e-3(3.02e-6)−	1.2722e-2(8.74e-5)	
+/−/≈		4/15/3	7/13/2	10/10/2	4/16/2		
DTLZ5	5	2.3258e-1(3.41e-3)+	1.7923e-1(3.53e-2)−	1.7708e-1(1.33e-2)−	1.6313e-1(3.41e-3)−	2.2180e-1(5.48e-3)	Irregular
	10	1.7579e-1(8.07e-3)≈	2.2389e-2(1.91e-2)−	1.1291e-1(1.30e-2)−	9.9083e-2(2.19e-2)−	1.7582e-1(6.76e-3)	
DTLZ6	5	2.2158e-1(1.19e-2)−	1.2083e-1(6.18e-2)−	1.9873e-1(3.29e-2)−	1.5605e-1(3.93e-2)−	2.3599e-1(8.09e-3)	
	10	1.5418e-1(4.07e-2)−	0.0000e+0(0.00e+0)−	1.3585e-1(3.52e-2)−	1.0801e-1(2.00e-2)−	1.9244e-1(1.05e-2)	
DTLZ7	5	9.0909e-2(4.94e-7)−	2.4167e-1(4.33e-3)+	2.0007e-1(9.91e-3)−	2.5327e-1(9.01e-3)+	2.3599e-1(2.48e-3)	
	10	1.1971e-3(3.11e-4)−	1.9584e-1(1.26e-2)+	1.4380e-1(1.51e-2)≈	1.6845e-1(1.72e-2)+	1.4646e-1(7.03e-3)	
IDTLZ1	5	3.0778e-3(1.34e-3)−	3.8005e-3(6.07e-4)−	2.5034e-3(9.68e-4)−	5.4947e-3(1.56e-4)−	1.0125e-2(2.65e-4)	
	10	3.6627e-8(1.09e-8)−	5.5700e-7(9.79e-8)−	1.1353e-8(7.35e-9)−	1.5082e-7(2.11e-8)−	8.1125e-7(3.78e-7)	
IDTLZ2	5	7.4532e-2(5.82e-4)−	6.2640e-2(7.15e-3)−	6.2911e-2(1.67e-3)−	4.7324e-2(4.73e-4)−	9.4761e-2(1.65e-3)	
	10	8.5413e-5(7.78e-6)−	1.2654e-4(3.09e-5)−	1.2274e-4(1.28e-5)−	1.5639e-4(1.72e-5)−	2.5020e-4(2.04e-5)	
WFG1	5	7.7075e-1(5.71e-2)−	7.8837e-1(3.33e-2)−	8.6621e-1(4.04e-2)−	9.6909e-1(4.51e-2)+	9.0787e-1(2.65e-2)	
	10	9.8947e-1(2.24e-2)+	7.0682e-1(4.79e-2)−	9.8712e-1(2.83e-2)+	9.9956e-1(2.12e-4)+	9.4718e-1(3.69e-2)	
WFG2	5	9.6933e-1(4.70e-3)−	9.9246e-1(1.19e-3)−	9.8809e-1(1.99e-3)−	9.9446e-1(1.51e-3)≈	9.9469e-1(5.81e-4)	
	10	9.6285e-1(6.50e-3)−	9.9671e-1(1.69e-3)+	9.8615e-1(3.22e-3)−	9.8719e-1(1.36e-2)−	9.9508e-1(1.06e-3)	
WFG3	5	5.8763e-1(1.40e-2)−	6.0849e-1(9.55e-3)−	5.9583e-1(1.53e-2)−	5.1206e-1(1.46e-2)−	6.1225e-1(6.30e-3)	
	10	4.7366e-1(1.46e-2)≈	6.5001e-1(1.78e-2)+	2.6506e-1(5.35e-2)−	1.9463e-1(8.06e-3)−	4.6749e-1(1.09e-2)	
MaF2	5	1.3682e-1(1.87e-3)−	1.6459e-1(4.26e-3)−	1.6226e-1(2.38e-3)−	1.0657e-1(2.06e-3)−	1.7203e-1(1.67e-3)	
	10	1.7154e-1(1.78e-3)−	2.1617e-1(5.48e-3)+	1.6992e-1(3.81e-3)−	1.1547e-1(3.15e-2)−	2.0725e-1(2.78e-3)	
MaF4	5	3.4357e-2(2.92e-3)−	5.0828e-2(1.97e-2)−	2.1837e-2(8.68e-3)−	4.3138e-2(4.99e-3)−	7.5395e-2(4.93e-3)	
	10	1.1488e-7(2.54e-8)−	2.6065e-4(2.98e-5)+	1.6017e-7(2.42e-7)−	1.2257e-4(1.44e-5)+	5.5956e-6(2.42e-6)	
MaF13	5	1.5248e-1(8.16e-2)−	2.1458e-1(1.23e-2)−	1.7354e-1(4.09e-2)−	1.5966e-1(4.48e-2)−	2.5982e-1(4.17e-3)	
	10	4.4595e-2(7.89e-3)−	1.1507e-1(7.90e-3)−	7.6784e-2(2.36e-2)−	1.0099e-1(1.16e-3)−	1.3705e-1(2.10e-3)	
+/−/≈		2/18/2	6/16/0	1/20/1	5/16/1		

'+', '−' and '≈' indicate that the result is significantly better, significantly worse and statistically similar to that obtained by AR-MOEA, respectively.

MaOPs with irregular Pareto fronts. For further observations, Fig. 9 plots the non-dominated solution set with the median HV value among 30 runs obtained by each algorithm on DTLZ1, IDTLZ1 and Pareto-Box problem with 10 objectives. It turns out that although all the five compared algorithms are able to obtain a solution set of good distribution on DTLZ1 which has a regular Pareto front, AR-MOEA is the only algorithm that has obtained a good approximation to irregular Pareto fronts such as IDTLZ1. Besides, as indicated by the Pareto-Box problem, AR-MOEA has also maintained better population diversity than the other four MOEAs. Since the Pareto optimal solutions of the Pareto-box problem are designed to be inside one (or several) two-dimensional closure(s) in the decision space, the candidate solutions outside the Pareto box (e.g. those obtained by NSGA-III and AR-MOEA) are thereby non-Pareto optimal. This is due to the fact that the algorithms have failed to obtain the candidate solutions dominating these non-Pareto solutions, such that they cannot be eliminated via non-dominated sorting from the final solution set. In general, without any modification or change in parameter setting, the proposed AR-MOEA has promising versatility in the optimization of MaOPs with various Pareto fronts.

TABLE V
IGD VALUES OBTAINED BY NSGA-III USING THE REFERENCE POINT ADAPTIVE METHODS DEVELOPED IN A-NSGA-III, RVEA* AND AR-MOEA ON DTLZ1, DTLZ3, DTLZ6 AND IDTLZ1 WITH 3, 5 AND 10 OBJECTIVES. THE BEST RESULT ON EACH TEST INSTANCE IS HIGHLIGHTED.

Problem	Obj.	A-NSGA-III	R-NSGA-III	AR-NSGA-III
DTLZ1	3	2.3434e-2−	2.8841e-2−	1.8931e-2
	5	6.3446e-2−	7.1247e-2−	6.2861e-2
	10	1.7341e-1−	2.5566e-1−	1.4292e-1
DTLZ3	3	6.8590e-2−	7.2553e-2−	5.0276e-2
	5	2.0753e-1−	2.8049e-1−	1.9531e-1
	10	2.0584e+0−	6.9093e-1−	4.9583e-1
DTLZ6	3	1.1305e-2−	9.2616e-3−	4.6882e-3
	5	5.1493e-1≈	3.8782e-1+	5.0407e-1
	10	4.8122e+0−	2.1881e+0+	3.1327e+0
IDTLZ1	3	7.0615e-2−	7.9936e-2−	6.6269e-2
	5	3.3223e-1−	4.1887e-1−	2.8802e-1
	10	1.2912e+0−	1.2808e+0−	1.2221e+0
+/ − / ≈		0/11/1	2/10/0	

'+', '−' and '≈' indicate that the result is significantly better, significantly worse and statistically similar to that obtained by AR-NSGA-III, respectively.

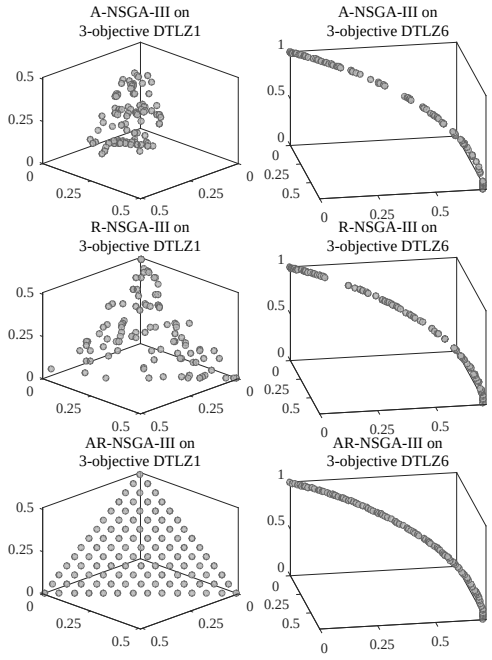

Fig. 10. The non-dominated solution set with the median IGD value among 30 runs obtained by NSGA-III using the reference point adaptation methods developed in A-NSGA-III, RVEA* and AR-MOEA on DTLZ1 and DTLZ6 with 3 objectives.

C. Effectiveness of the Proposed Reference Point Adaptation Method

In this subsection, we assess the performance of the proposed reference point adaptation method by comparing it with two reference point adaptation methods developed in A-NSGA-III and RVEA*. For fair comparisons, we embed these reference point adaptation methods into the same MOEA, namely, NSGA-III. For simplicity, the NSGA-III using the reference point adaptation methods in A-NSGA-III, RVEA* and AR-MOEA are hereafter denoted as A-NSGA-III, R-NSGA-III and AR-NSGA-III, respectively.

Table V presents the IGD values obtained by the three compared algorithms on DTLZ1, DTLZ3, DTLZ6 and IDTLZ1 with 3, 5 and 10 objectives, where there are three observations that can be made. First, the proposed reference point adaptation method performs much better than the two compared methods on DTLZ1 and DTLZ3 in terms of IGD values. By contrast, the reference point adaptation methods adopted in A-NSGA-III and RVEA*, which are specially designed for solving problems with irregular Pareto fronts, fail to handle regular Pareto fronts very well.

Second, the proposed reference point adaptation method also shows competitive performance on DTLZ6 and IDTLZ1, both of which have irregular Pareto fronts. It is worth noting that, however, on DTLZ6 with more than three objectives, the proposed adaptation method is slightly outperformed by that developed in RVEA*. This is mainly due to the fact that NSGA-III has difficulty in convergence on DTLZ6, such that the adaptation method proposed in AR-MOEA fails to adjust the reference points properly according to the archived candidate solutions.

To further observe the differences between solution sets obtained by the three compared adaptation methods, Fig. 10 depicts the objective values of non-dominated solution set with a median IGD value among 30 runs. It can be clearly seen that the proposed reference point adaptation method outperforms the adaptation methods suggested in A-NSGA-III and RVEA* on both DTLZ1 and DTLZ6, which have a regular and irregular Pareto front, respectively.

On the basis of the empirical observations above, we can conclude that the proposed reference point adaptation method still performs well when embedded in other decomposition based MOEAs such as NSGA-III, regardless of the Pareto front shapes of the problems to be solved.

D. Sensitivity Analysis of Population Size

In all the experiments above, the population size is always set to the same as the number of reference points in the decomposition based algorithms such as MOEA/D and NSGA-III. This is due to the fact that, in decomposition based MOEAs, each reference point is often associated with a unique candidate solution, and the specific number of reference points is determined by the Das and Dennis's systematic approach [48].

As discussed in Section III-D, by contrast, the proposed AR-MOEA provides a more flexible way for population size setting, where the number of candidate solutions can be an arbitrary number smaller than the number of reference points. Some empirical experiments are conducted on 3-objective DTLZ3 and DTLZ6 using AR-MOEA with different population sizes. Fig. 11 presents the non-dominated solution set with the median IGD

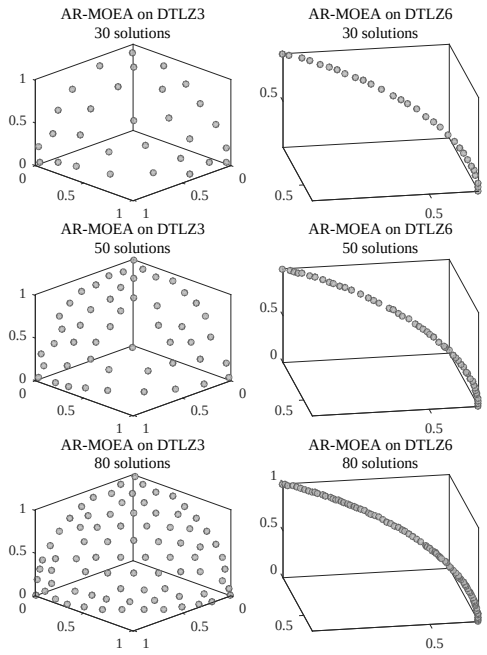

Fig. 11. The non-dominated solution set with the median IGD value among 30 runs obtained by the AR-MOEA with the population size of 30, 50 and 80 on DTLZ3 and DTLZ6 with 3 objectives, where the number of reference points is always set to 105.

value among 30 runs obtained by the AR-MOEA with population sizes of 30, 50 and 80 on DTLZ3 and DTLZ6 with three objectives, where the number of reference points is always set to 105. It can be seen that, the distribution of the non-dominated solution set obtained by AR-MOEA is always adaptively adjusted regardless of the specific population size, which provides a good flexibility for population size setting. It is worth noting that, however, if the population size is larger than the number of reference points, due to the lack of reference points, there will be duplicate candidate solutions at the same positions, such that the unique candidate solutions in the final solution is still identical to the number of given reference points.

V. Conclusions and Remarks

In this paper, we have proposed an enhanced inverted generational distance (IGD-NS) based MOEA with reference point adaptation, termed AR-MOEA, for solving both MOPs and MaOPs with various types of Pareto fronts. In order to improve the versatility of the proposed AR-MOEA, a reference point adaptation method has been developed to adjust the reference points at each generation for the indicator calculation. In the proposed adaptation method, the reference points are adapted on the basis of an initialized reference point set together with candidate solutions stored in an external archive based on their contributions to the IGD-NS indicator, thus taking both uniform distribution and Pareto front approximation into consideration. In addition, this reference point adaptation method is parameterless, and can be easily deployed in other existing decomposition based MOEAs to improve their performance on problems with irregular Pareto fronts.

Empirical results have demonstrated that the proposed AR-MOEA outperforms eight representative MOEAs on both MOPs and MaOPs with various types of Pareto fronts, showing promising versatility. Performance of the proposed reference point adaptation method has been further assessed by embedding it into NSGA-III. In comparison with another two state-of-the-art adaptation methods, the proposed method still shows the best performance on problems with both regular and irregular Pareto fronts.

The proposed AR-MOEA has demonstrated that the IGD-NS is a promising performance indicator in designing versatile MOEAs for solving MOPs and MaOPs. However, further investigation of applying IGD-NS in other MOEAs is still desirable, especially on problems with a large number of decision variables, namely, large-scale MOPs or MaOPs [47], [61]. Besides, we would also like to further investigate how to handle more challenging problems where parts of Pareto fronts cannot be easily obtained during the search process. This will probably call for the development of new reproduction operators.

References

[1] A. Zhou, B.-Y. Qu, H. Li, S.-Z. Zhao, P. N. Suganthan, and Q. Zhang, "Multiobjective evolutionary algorithms: A survey of the state of the art," *Swarm and Evolutionary Computation*, vol. 1, no. 1, pp. 32–49, 2011.

[2] B. Li, J. Li, K. Tang, and X. Yao, "Many-objective evolutionary algorithms: A survey," *ACM Computing Surveys*, vol. 48, no. 1, p. 13, 2015.

[3] K. Deb, A. Pratap, S. Agarwal, and T. Meyarivan, "A fast and elitist multi-objective genetic algorithm: NSGA-II," *IEEE Transactions on Evolutionary Computation*, vol. 6, no. 2, pp. 182–197, 2002.

[4] E. Zitzler, M. Laumanns, and L. Thiele, "SPEA2: Improving the strength Pareto evolutionary algorithm for multiobjective optimization," in *Proceedings of the Fifth Conference on Evolutionary Methods for Design, Optimization and Control with Applications to Industrial Problems*, 2001, pp. 95–100.

[5] D. W. Corne, N. R. Jerram, J. D. Knowles, and M. J. Oates, "PESA-II: Region-based selection in evolutionary multi-objective optimization," in *Proceedings of the 2001 Conference on Genetic and Evolutionary Computation*, 2001, pp. 283–290.

[6] R. C. Purshouse and P. J. Fleming, "On the evolutionary optimization of many conflicting objectives," *IEEE Transactions on Evolutionary Computation*, vol. 11, no. 6, pp. 770–784, 2007.

[7] S. Yang, M. Li, X. Liu, and J. Zheng, "A grid-based evolutionary algorithm for many-objective optimization," *IEEE Transactions on Evolutionary Computation*, vol. 17, no. 5, pp. 721–736, 2013.

[8] X. Zhang, Y. Tian, and Y. Jin, "A knee point driven evolutionary algorithm for many-objective optimization," *IEEE Transactions on Evolutionary Computation*, vol. 19, no. 6, pp. 761–776, 2014.

[9] H. Ishibuchi and T. Murata, "A multi-objective genetic local search algorithm and its application to flowshop scheduling," *IEEE Transactions on Systems, Man, and Cybernetics, Part C: Applications and Reviews*, vol. 28, no. 3, pp. 392–403, 1998.

[10] T. Murata, H. Ishibuchi, and M. Gen, "Specification of genetic search directions in cellular multi-objective genetic algorithms," in *Proceedings of First International Conference on Evolutionary Multi-Criterion Optimization*, 2001, pp. 82–95.

[11] E. J. Hughes, "MSOPS-II: A general-purpose many-objective optimiser," in *Proceedings of the 2007 IEEE Congress on Evolutionary Computation*, 2007, pp. 3944–3951.

[12] Q. Zhang and H. Li, "MOEA/D: A multi-objective evolutionary algorithm based on decomposition," *IEEE Transactions on Evolutionary Computation*, vol. 11, no. 6, pp. 712–731, 2007.

[13] R. Cheng, Y. Jin, M. Olhofer, and B. Sendhoff, "A reference vector guided evolutionary algorithm for many-objective optimization," *IEEE Transactions on Evolutionary Computation*, vol. 20, no. 5, pp. 773–791, 2016.

[14] H.-L. Liu, F. Gu, and Q. Zhang, "Decomposition of a multiobjective optimization problem into a number of simple multiobjective subproblems," *IEEE Transactions on Evolutionary Computation*, vol. 18, no. 3, pp. 450–455, 2014.

[15] R. Cheng, Y. Jin, K. Narukawa, and B. Sendhoff, "A multiobjective evolutionary algorithm using Gaussian process based inverse modeling," *IEEE Transactions on Evolutionary Computation*, vol. 19, no. 6, pp. 838–856, 2015.

[16] K. Deb and H. Jain, "An evolutionary many-objective optimization algorithm using reference-point based non-dominated sorting approach, part I: Solving problems with box constraints," *IEEE Transactions on Evolutionary Computation*, vol. 18, no. 4, pp. 577–601, 2014.

[17] S. Jiang and S. Yang, "A strength Pareto evolutionary algorithm based on reference direction for multi-objective and many-objective optimization," *IEEE Transactions on Evolutionary Computation*, 2016, in press.

[18] E. Zitzler and S. Künzli, "Indicator-based selection in multiobjective search," in *Proceedings of the 8th International Conference on Parallel Problem Solving from Nature*, 2004, pp. 832–842.

[19] N. Beume, B. Naujoks, and M. Emmerich, "SMS-EMOA: Multiobjective selection based on dominated hypervolume," *European Journal of Operational Research*, vol. 181, no. 3, pp. 1653–1669, 2007.

[20] A. Menchaca-Mendez and C. A. Coello Coello, "GDE-MOEA: A new moea based on the generational distance indicator and ϵ-dominance," in *Proceedings of the 2015 IEEE Congress on Evolutionary Computation*, 2015, pp. 947–955.

[21] R. Hernández Gómez and C. A. Coello Coello, "Improved metaheuristic based on the R2 indicator for many-objective optimization," in *Proceedings of the 2015 International Conference on Genetic and Evolutionary Computation*, 2015, pp. 679–686.

[22] J. Bader and E. Zitzler, "HypE: An algorithm for fast hypervolume-based many-objective optimization," *Evolutionary Computation*, vol. 19, no. 1, pp. 45–76, 2011.

[23] I. Yevseyeva, A. P. Guerreiro, M. T. Emmerich, and C. M. Fonseca, "A portfolio optimization approach to selection in multiobjective evolutionary algorithms," in *Proceedings of International Conference on Parallel Problem Solving from Nature*, 2014, pp. 672–681.

[24] A. P. Guerreiro and C. M. Fonseca, "Hypervolume Sharpe-Ratio indicator: Formalization and first theoretical results," in *Proceedings of International Conference on Parallel Problem Solving from Nature*, 2016, pp. 814–823.

[25] M. Li, S. Yang, and X. Liu, "Pareto or non-Pareto: Bi-criterion evolution in multi-objective optimization," *IEEE Transactions on Evolutionary Computation*, vol. 20, no. 5, pp. 645–665, 2016.

[26] H. Ishibuchi, Y. Setoguchi, H. Masuda, and Y. Nojima, "Performance of decomposition-based many-objective algorithms strongly depends on Pareto front shapes," *IEEE Transactions on Evolutionary Computation*, 2016, in press.

[27] Y. Tian, X. Zhang, R. Cheng, and Y. Jin, "A multi-objective evolutionary algorithm based on an enhanced inverted generational distance metric," in *Proceedings of the 2016 IEEE Congress on Evolutionary Computation*, 2016, pp. 5222–5229.

[28] D. A. V. Veldhuizen and G. B. Lamont, "Multiobjective evolutionary algorithm research: A history and analysis," Department of Electrical and Computer Engineering. Graduate School of Engineering, Air Force Inst Technol, Wright Patterson, Tech. Rep. TR-98-03, Tech. Rep., 1998.

[29] A. Zhou, Y. Jin, Q. Zhang, B. Sendhoff, and E. Tsang, "Combining model-based and genetics-based offspring generation for multi-objective optimization using a convergence criterion," in *Proceedings of the 2006 IEEE Congress on Evolutionary Computation*, 2006, pp. 892–899.

[30] L. While, P. Hingston, L. Barone, and S. Huband, "A faster algorithm for calculating hypervolume," *IEEE Transactions on Evolutionary Computation*, vol. 10, no. 1, pp. 29–38, 2006.

[31] D. Brockhoff, T. Wagner, and H. Trautmann, "On the properties of the R2 indicator," in *Proceedings of the 14th Annual Conference on Genetic and Evolutionary Computation*, 2012, pp. 465–472.

[32] O. Schütze, X. Esquivel, A. Lara, and C. A. C. Coello, "Using the averaged hausdorff distance as a performance measure in evolutionary multiobjective optimization," *IEEE Transactions on Evolutionary Computation*, vol. 16, no. 4, pp. 504–522, 2012.

[33] H. Wang, Y. Jin, and X. Yao, "Diversity assessment in many-objective optimization," *IEEE Transactions on Cybernetics*, 2016, in press.

[34] H. Trautmann, T. Wagner, and D. Brockhoff, "R2-EMOA: Focused multiobjective search using R2-indicator-based selection," in *Proceedings of the 7th International Conference on Learning and Intelligent Optimization*, 2013, pp. 70–74.

[35] R. H. Gómez and C. A. C. Coello, "MOMBI: A new metaheuristic for many-objective optimization based on the R2 indicator," in *Proceedings of the 2013 IEEE Congress on Evolutionary Computation*, 2013, pp. 2488–2495.

[36] A. Menchaca-Mendez and C. A. C. Coello, "GD-MOEA: A new multi-objective evolutionary algorithm based on the generational distance indicator," in *Proceedings of the 8th International Conference on Evolutionary Multi-Criterion Optimization*, 2015, pp. 156–170.

[37] G. Rudolph, O. Schütze, C. Grimme, and H. Trautmann, "An aspiration set EMOA based on averaged hausdorff distances," in *Proceedings of the 8th International Conference on Learning and Intelligent Optimization*, 2014, pp. 153–156.

[38] K. Gerstl, G. Rudolph, O. Schütze, and H. Trautmann, "Finding evenly spaced fronts for multiobjective control via averaging hausdorff-measure," in *Proceedings of the 8th International Conference on Electrical Engineering Computing Science and Automatic Control*, 2011, pp. 1–6.

[39] H. Trautmann, G. Rudolph, C. Dominguez-Medina, and O. Schütze, "Finding evenly spaced Pareto fronts for three-objective optimization problems," in *EVOLVE-A Bridge between Probability, Set Oriented Numerics, and Evolutionary Computation II*. Springer, 2013, pp. 89–105.

[40] G. Rudolph, H. Trautmann, S. Sengupta, and O. Schütze, "Evenly spaced Pareto front approximations for tricriteria problems based on triangulation," in *Proceedings of 8th International Conference on Evolutionary Multi-Criterion Optimization*, 2013, pp. 443–458.

[41] Y. Qi, X. Ma, F. Liu, L. Jiao, J. Sun, and J. Wu, "MOEA/D with adaptive weight adjustment," *Evolutionary computation*, vol. 22, no. 2, pp. 231–264, 2014.

[42] R. Cheng, Y. Jin, and K. Narukawa, "Adaptive reference vector generation for inverse model based evolutionary multiobjective optimization with degenerate and disconnected Pareto fronts," in *Proceedings of the 8th International Conference on Evolutionary Multi-Criterion Optimization*, 2015, pp. 127–140.

[43] H. Jain and K. Deb, "An evolutionary many-objective optimization algorithm using reference-point based nondominated sorting approach, part II: Handling constraints and extending to an adaptive approach," *IEEE Transactions on Evolutionary Computation*, vol. 18, no. 4, pp. 602–622, 2014.

[44] H. Li and D. Landa-Silva, "An adaptive evolutionary multi-objective approach based on simulated annealing," *Evolutionary Computation*, vol. 19, no. 4, pp. 561–595, 2011.

[45] S. Jiang, Z. Cai, J. Zhang, and Y.-S. Ong, "Multiobjective optimization by decomposition with Pareto-adaptive weight vectors," in *Proceedings of the Seventh International Conference on Natural Computation*, vol. 3, 2011, pp. 1260–1264.

[46] X. Zhang, Y. Tian, R. Cheng, and Y. Jin, "An efficient approach to non-dominated sorting for evolutionary multi-objective optimization," *IEEE Transactions on Evolutionary Computation*, vol. 19, no. 2, pp. 201–213, 2015.

[47] X. Zhang, Y. Tian, R. Cheng, and Y. . Jin, "A decision variable clustering-based evolutionary algorithm for large-scale many-objective optimization," *IEEE Transactions on Evolutionary Computation*, 2016, in press.

[48] I. Das and J. E. Dennis, "Normal-boundary intersection: A new method for generating the Pareto surface in nonlinear multicriteria optimization problems," *SIAM Journal on Optimization*, vol. 8, no. 3, pp. 631–657, 1998.

[49] C. He, L. Pan, H. Xu, Y. Tian, and X. Zhang, "An improved reference point sampling method on Pareto optimal front," in *Proceedings of the 2016 IEEE Congress on Evolutionary Computation*, 2016, pp. 5230–5237.

[50] L. B. S. Huband, P. Hingston and L. While, "A review of multi-objective test problems and a scalable test problem toolkit," *IEEE Transactions on Evolutionary Computation*, vol. 10, no. 5, pp. 477–506, 2006.

[51] D. K. Saxena, J. A. Duro, A. Tiwari, K. Deb, and Q. Zhang, "Objective reduction in many-objective optimization: Linear and nonlinear algorithms," *IEEE Transactions on Evolutionary Computation*, vol. 17, no. 1, pp. 77–99, 2013.
[52] H. Ishibuchi, H. Masuda, and Y. Nojima, "Pareto fronts of many-objective degenerate test problems," *IEEE Transactions on Evolutionary Computation*, vol. 20, no. 5, pp. 807–813, 2016.
[53] K. Li, K. Deb, Q. Zhang, and S. Kwong, "Combining dominance and decomposition in evolutionary many-objective optimization," *IEEE Transactions on Evolutionary Computation*, vol. 19, no. 5, pp. 694–716, 2015.
[54] K. Deb, L. Thiele, M. Laumanns, and E. Zitzler, *Scalable test problems for evolutionary multiobjective optimization*. Springer, 2005.
[55] R. Cheng, M. Li, Y. Tian, X. Zhang, S. Yang, Y. Jin, and X. Yao, "Benchmark functions for the CEC'2017 competition on many-objective optimization," Technical Report No. CSR-17-01, School of Computer Science, University of Birmingham, Tech. Rep., 2017.
[56] M. Köppen and K. Yoshida, "Substitute distance assignments in NSGA-II for handling many-objective optimization problems," in *Proceedings of the 4th International Conference on Evolutionary Multi-Criterion Optimization*, 2007, pp. 727–741.
[57] H. Li, Q. Zhang, and J. Deng, "Biased multiobjective optimization and decomposition algorithm," *IEEE Transactions on Cybernetics*, vol. 47, no. 1, pp. 52–66, 2017.
[58] K. Deb, *Multi-Objective Optimization Using Evolutionary Algorithms*. New York: Wiley, 2001.
[59] K. Deb and M. Goyal, "A combined genetic adaptive search (GeneAS) for engineering design," *Computer Science and Informatics*, vol. 26, no. 4, pp. 30–45, 1996.
[60] M. Li, S. Yang, and X. Liu, "Shift-based density estimation for Pareto-based algorithms in many-objective optimization," *IEEE Transactions on Evolutionary Computation*, vol. 18, no. 3, pp. 348–365, 2014.
[61] X. Ma, F. Liu, Y. Qi, X. Wang, L. Li, L. Jiao, M. Yin, and M. Gong, "A multiobjective evolutionary algorithm based on decision variable analyses for multi-objective optimization problems with large scale variables," *IEEE Transactions on Evolutionary Computation*, vol. 20, no. 2, pp. 275–298, 2016.